

## RESEARCH ARTICLE

# RPTP $\alpha$ controls epithelial adherens junctions, linking E-cadherin engagement to c-Src-mediated phosphorylation of cortactin

Marta Truffi<sup>1</sup>, Véronique Dubreuil<sup>1,§</sup>, Xuan Liang<sup>2</sup>, Nathalie Vacaresse<sup>3,\*</sup>, Fabienne Nigon<sup>1</sup>, Siew Ping Han<sup>2,‡</sup>, Alpha S. Yap<sup>2</sup>, Guillermo A. Gomez<sup>2</sup> and Jan Sap<sup>1,3,§</sup>

## ABSTRACT

Epithelial junctions are fundamental determinants of tissue organization, subject to regulation by tyrosine phosphorylation. Homophilic binding of E-cadherin activates tyrosine kinases, such as Src, that control junctional integrity. Protein tyrosine phosphatases (PTPs) also contribute to cadherin-based adhesion and signaling, but little is known about their specific identity or functions at epithelial junctions. Here, we report that the receptor PTP RPTP $\alpha$  (human gene name *PTPRA*) is recruited to epithelial adherens junctions at the time of cell–cell contact, where it is in molecular proximity to E-cadherin. RPTP $\alpha$  is required for appropriate cadherin-dependent adhesion and for cyst architecture in three-dimensional culture. Loss of RPTP $\alpha$  impairs adherens junction integrity, as manifested by defective E-cadherin accumulation and peri-junctional F-actin density. These effects correlate with a role for RPTP $\alpha$  in cellular (c)-Src activation at sites of E-cadherin engagement. Mechanistically, RPTP $\alpha$  is required for appropriate tyrosine phosphorylation of cortactin, a major Src substrate and a cytoskeletal actin organizer. Expression of a phosphomimetic cortactin mutant in RPTP $\alpha$ -depleted cells partially rescues F-actin and E-cadherin accumulation at intercellular contacts. These findings indicate that RPTP $\alpha$  controls cadherin-mediated signaling by linking homophilic E-cadherin engagement to cortactin tyrosine phosphorylation through c-Src.

**KEY WORDS:** E-cadherin, Adherens junctions, Tyrosine phosphatase, Cortactin, c-Src

## INTRODUCTION

Cadherin-based epithelial junctions are fundamental determinants of tissue organization, dysfunction of which is associated with multiple pathologies. They mediate intercellular adhesion through the homophilic binding of E-cadherin and its interaction with the actin cytoskeleton (Harris and Tepass, 2010; Mège et al., 2006).

Diverse signaling pathways, such as those involving protein tyrosine phosphorylation and small G proteins, contribute to junction assembly, remodeling and turnover (Braga and Yap, 2005; Maher et al., 1985; McLachlan and Yap, 2007; Nelson, 2008). Locally accumulated tyrosine kinases of the Src family (Src family kinases; SFKs) are activated in response to homophilic binding of E-cadherin at the cell–cell interface (McLachlan et al., 2007), participate in signal transmission and regulate junctional properties. Inhibition of cellular (c)-Src activity significantly perturbs E-cadherin distribution, homophilic adhesion and actin cytoskeleton organization (Calautti et al., 1998; Takahashi et al., 2005). At the same time, constitutively active viral (v)-Src also disrupts the integrity of cell–cell contacts, impairing contact formation and extension (Behrens et al., 1993; Volberg et al., 1991; Warren and Nelson, 1987). Clearly, SFK signaling can both positively and negatively affect E-cadherin function, depending on the SFK signal strength (McLachlan et al., 2007). The complexity of SFK functions at cadherin-based junctions makes it necessary to identify the SFK regulators at this cellular locale, so as to understand how SFKs are affected by locally received signals, such as cell–cell contact or mechanical force.

Among other regulatory mechanisms, Src kinases are subject to regulation through phosphorylation of a number of discrete tyrosine residues, with positive or negative effects on kinase activity (Roskoski, 2005). Recent data also point to a role for protein tyrosine phosphatase (PTP) activity in the maintenance of intercellular junction integrity. Inhibition of PTP activity by pervanadate treatment disrupts epithelial junctions and, interestingly, impairs E-cadherin-activated Src signaling (McLachlan and Yap, 2011). Although some studies have reported a role for cell-contact-associated PTPs in controlling the integrity and function of epithelial junctions (Anders et al., 2006; Espejo et al., 2010; Fuchs et al., 1996; Müller et al., 1999; Sheth et al., 2007), none of the identified PTPs has been shown to control junctional SFKs.

Here, we report that the transmembrane receptor protein tyrosine phosphatase RPTP $\alpha$  (human gene name *PTPRA*), a well-established physiological regulator of c-Src (Ponniah et al., 1999; Su et al., 1999), localizes to intercellular junctions in epithelial cells and is required for their integrity. RPTP $\alpha$  is already known to participate in fibroblastic adhesion-mediated processes, such as integrin-dependent spreading, cell motility and force transduction at integrin–cytoskeleton linkages (Jiang et al., 2006; Su et al., 1999; von Wichert et al., 2003), and to function with various neuronal cell adhesion molecules in neurons (Bodrikov et al., 2005; Ye et al., 2008). PTPs are now recognized to affect cell behaviors related to oncogenicity in complex ways (Labbé et al., 2012). Overexpression of RPTP $\alpha$  can induce fibroblast transformation, presumably through its Src-activating activity (Tremper-Wells et al., 2010;

<sup>1</sup>Université Paris Diderot, Sorbonne Paris Cité, Epigenetics and Cell Fate, UMR 7216 CNRS, Bâtiment Lamarck, Case 7042, 35 Rue Hélène Brion, F-75205 Paris Cedex 13, France. <sup>2</sup>Division of Molecular Cell Biology, Institute for Molecular Bioscience, University of Queensland, St. Lucia, Brisbane 4072, Australia.

<sup>3</sup>Biotech Research and Innovation Centre and Department of Biomedical Sciences, Faculty of Health Sciences, University of Copenhagen, Ole Maaløes Vej 5, 2200 Copenhagen N, Denmark.

\*Present address: Department of Immunology, The University of Toronto, Sunnybrook Research Institute, 2075 Bayview Avenue, Toronto, ON M4N 3M5, Canada. †Present address: Centre for BioImaging Sciences, National University of Singapore, 14 Science Drive 4, S1A Level 2, 117557 Singapore.

§Authors for correspondence (veronique.dubreuil@univ-paris-diderot.fr; jansap@fastmail.fm)

Zheng et al., 1992). Although *in vitro* and *in vivo* observations indicate that RPTP $\alpha$  can also control carcinoma tumorigenesis and/or invasiveness (Ardini et al., 2000; Huang et al., 2011; Krndija et al., 2010; Meyer et al., 2013), its cell biological function in the epithelial context has hardly been investigated. Identifying RPTP $\alpha$  as a mediator of E-cadherin-dependent c-Src activation provides new insight into the relevance of receptor PTPs for the properties of normal and neoplastic epithelia.

## RESULTS

### RPTP $\alpha$ localizes to cadherin-based intercellular junctions in epithelial cells, and is in molecular proximity to E-cadherin

To start investigating the intracellular localization of RPTP $\alpha$  in the epithelial context, we expressed a fusion protein between human RPTP $\alpha$  and the fluorescent protein Venus (Nagai et al., 2002) in various epithelial cell lines. This revealed a striking pattern of accumulation of RPTP $\alpha$  at cell–cell junctions

(Fig. 1A). In order to document the kinetics of this localization, we followed the process of formation of cell–cell contacts by time-lapse imaging. We noticed that RPTP $\alpha$  was recruited to intercellular adhesion sites from the early stages of contact formation, when lamellipodial protrusions from two cells touched one another, and that it subsequently remained at local contact sites, accumulating along the cell–cell interface (Fig. 1B; supplementary material Movie 1).

To characterize the epithelial localization of RPTP $\alpha$ , we investigated its colocalization with junctional complexes, focusing on adherens junctions, marked by E-cadherin (Fig. 1C), and on tight junctions, marked by ZO-1 (Fig. 1D). Extensive overlap between RPTP $\alpha$  and E-cadherin was observed, whereas a different localization was detected with respect to ZO-1. We found that RPTP $\alpha$  colocalized with E-cadherin at the lateral membrane (Pearson's correlation coefficient  $r=0.7$ ); by contrast, RPTP $\alpha$  and ZO-1 clearly occupied distinct portions of

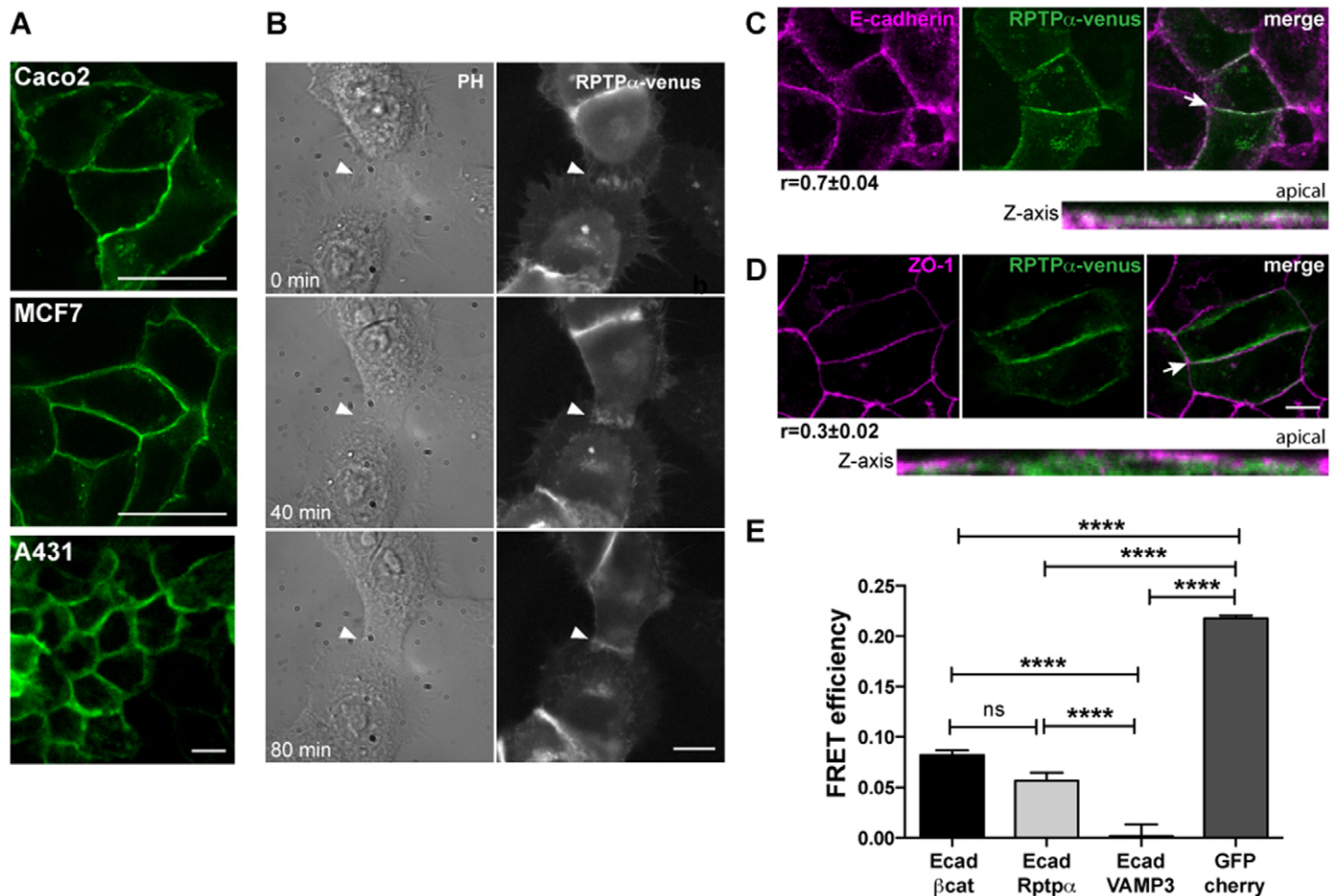


**Fig. 1. RPTP $\alpha$  localizes at the cadherin-based intercellular junctions in epithelial cells, where it is in close proximity to E-cadherin.** (A) Detection of Venus-tagged RPTP $\alpha$  in monolayer cultures of Caco-2, A431 and MCF7 cells. Scale bars: 20  $\mu$ m. (B) Time-lapse analysis of RPTP $\alpha$  during the establishment of cell–cell contacts. Intercellular contact formation was followed by using time-lapse video microscopy of A431 cells expressing Venus-tagged RPTP $\alpha$ . Phase-contrast (PH) and RPTP $\alpha$ –Venus epifluorescence images were acquired every 10 minutes, and selected time-points are shown. Arrowheads, RPTP $\alpha$  in early cell–cell contact establishment; Scale bar: 10  $\mu$ m. (C,D) Colocalization analysis of RPTP $\alpha$  with E-cadherin and ZO-1. Caco-2 cells expressing RPTP $\alpha$ –Venus (green) were immunolabeled for (C) E-cadherin or (D) ZO-1 (both purple) and analyzed by confocal microscopy. Single optical sections are shown. A z-axis view of individual contacts (following the direction of the arrow) illustrates the distribution of RPTP $\alpha$  and E-cadherin (C) or RPTP $\alpha$  and ZO-1 (D). Overlap between RPTP $\alpha$  and E-cadherin (C) or ZO-1 (D) at junctions ( $n=23$ , two independent experiments) was analyzed by calculation of Pearson's correlation coefficient ( $r$ ). Scale bar: 10  $\mu$ m. (E) FRET efficiency measurements in Caco-2 cells between E-cadherin and  $\beta$ -catenin (positive control); E-cadherin and RPTP $\alpha$ ; E-cadherin and vesicle-associated membrane protein-3 (VAMP3, negative control); and within a tandem GFP–Cherry fusion protein. Data show the mean  $\pm$  s.e.m., a representative of three independent experiments is shown;  $\sim 75$  cell–cell contacts. \*\*\*\* $P < 0.0001$ ; ns, not significant.

the membrane (Pearson's correlation  $r=0.3$ ), as also shown by the  $z$ -axis views. These data reveal that RPTP $\alpha$  specifically accumulates at adherens junctions, which are characterized by the presence of E-cadherin.

We then investigated whether RPTP $\alpha$  and E-cadherin might be in molecular proximity to one another. Co-immunoprecipitation experiments in Caco-2 cells revealed weak (130% relative to control) but significant ( $P=0.027$  in nine independent experiments; data not shown) enrichment of E-cadherin within anti-RPTP $\alpha$  immune complexes as compared with control IgG complexes. Subsequently, we measured fluorescence resonance energy transfer (FRET) between both molecules in live Caco-2 cells, using the E-cadherin/ $\beta$ -catenin and E-cadherin/VAMP3 pairs as positive and negative controls, respectively (Ferrari et al., 2012). This analysis revealed a FRET efficiency between RPTP $\alpha$  and E-cadherin at junctions that was similar to that between E-cadherin and  $\beta$ -catenin (Fig. 1E).

### RPTP $\alpha$ depletion compromises Caco-2 morphogenesis, and results in aberrant positioning of the apical compartment in 3D cultures

Adherens junctions are important determinants of epithelial tissue integrity and morphogenesis (Gumbiner, 2005; Halbleib and Nelson, 2006; Nishimura and Takeichi, 2009). To assess whether RPTP $\alpha$  is involved in epithelial organization, we examined whether it is required for the formation of cysts, typical three-dimensional (3D) structures generated by epithelial cells. When cultivated in a Matrigel matrix, Caco-2 cells assemble into ordered structures consisting of highly polarized cells interconnected by epithelial junctions (Jaffe et al., 2008). We compared cyst formation between pools of Caco-2 cells that had undergone stable lentiviral-induced knockdown of RPTP $\alpha$  and control Caco-2 cells expressing a non-targeting control shRNA. The two pools of RPTP $\alpha$ -knockdown cells retained different levels of residual RPTP $\alpha$  protein (Fig. 2A,B). Cyst formation was

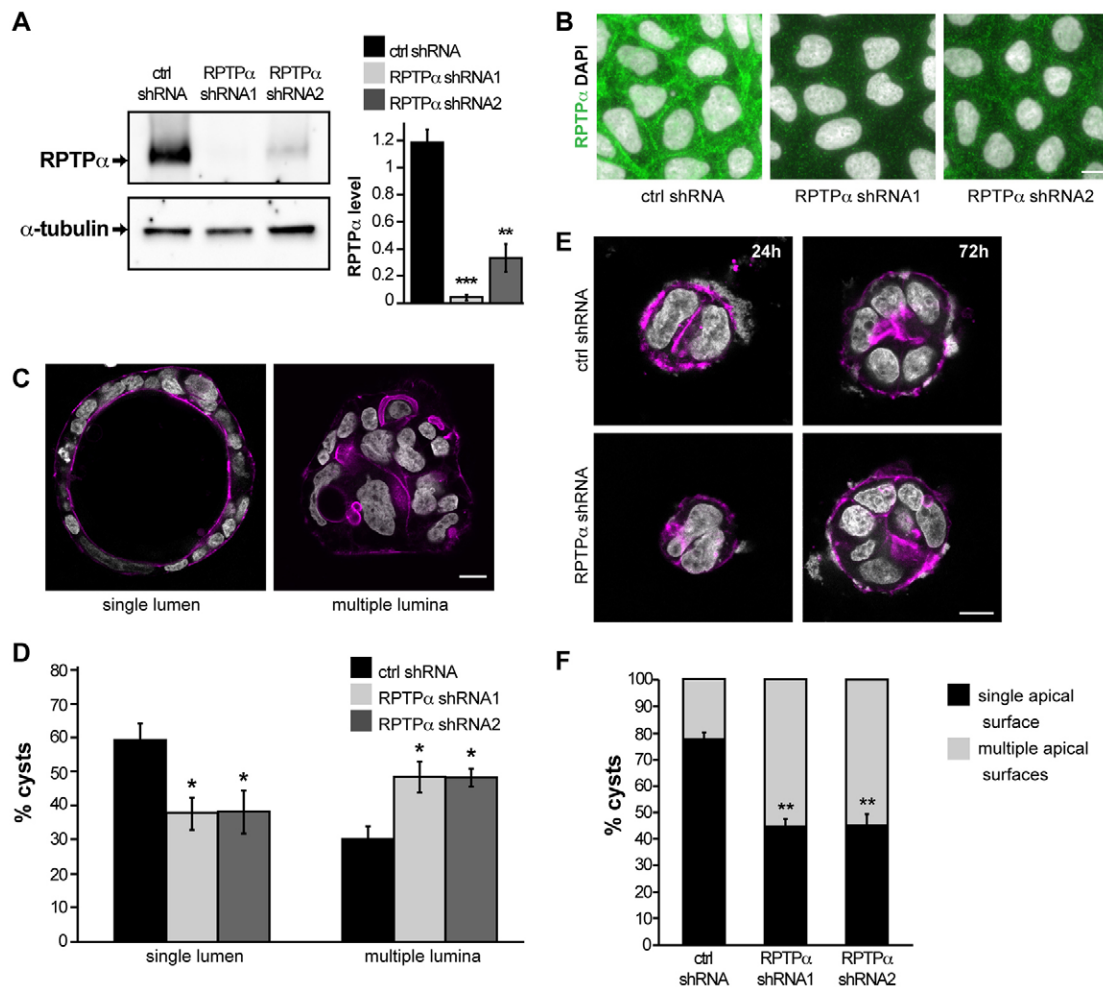


**Fig. 2. RPTP $\alpha$  depletion inhibits Caco-2 morphogenesis, and results in aberrant positioning of the apical compartment in 3D cultures.** Stable RPTP $\alpha$  knockdown (RPTP $\alpha$  shRNA1 and shRNA2) or control (ctrl shRNA) Caco-2 cells were generated by lentiviral infection. (A) Western blot analysis of RPTP $\alpha$  in control and RNAi-treated cells. Densitometric quantification of RPTP $\alpha$  levels normalized to  $\alpha$ -tubulin and compared with control is shown as the mean  $\pm$  s.e.m. (five independent experiments). (B) Immunofluorescence of RPTP $\alpha$  (green) in control and RPTP $\alpha$ -knockdown cells. Nuclei are stained with DAPI (white). Scale bar: 10  $\mu$ m. (C) Cysts formed after two weeks of culture in a Matrigel matrix. Representative confocal pictures of cysts with normal morphology (single central lumen) or with multiple lumina were obtained by immunofluorescence for F-actin (purple). Nuclei are stained with DAPI (white). Scale bar: 20  $\mu$ m. (D) Quantification of cysts with normal morphology or with multiple lumina in both control and RPTP $\alpha$ -knockdown cells is shown as the mean  $\pm$  s.e.m. (three independent experiments,  $n=100$ ). (E) Early stages (24 hours and 72 hours) of cyst formation in both control and RPTP $\alpha$ -knockdown cells. Immunostaining for actin was performed (purple); nuclei are stained with DAPI (white). Scale bar: 10  $\mu$ m. (F) Quantification of cysts with a central single apical surface or with multiple apical surfaces after 72 hours of culture in a Matrigel matrix. Data show the mean  $\pm$  s.e.m. (three independent experiments,  $n=100$ ). \* $P<0.05$ ; \*\* $P<0.01$ ; \*\*\* $P<0.001$ .



assessed after 14 days of culture, through emergence of a central lumen, as revealed by F-actin. Although the majority of control cells efficiently developed single-lumen cysts, RPTP $\alpha$ -depleted cysts more often appeared abnormal, with multiple lumina opening in various positions within the cyst. Quantification revealed that RPTP $\alpha$  depletion significantly increased the population of cysts with multiple lumina from 37% to 53% (Fig. 2C,D).

To gain insight into the mechanism by which RPTP $\alpha$  depletion resulted in multiple lumina, the effect of RPTP $\alpha$  knockdown on the development of cysts was also examined at early time points (24 and 72 hours after seeding). As expected, in control cells, a symmetrically placed F-actin-marked precursor apical surface appeared in the middle of the nascent cyst from the two-cell stage onward. As cysts grew, the single apical region was maintained at the center of the structure, where the lumen should progressively open (Fig. 2E, upper panels). By contrast, RPTP $\alpha$ -depleted cells often displayed a lateral shift of their apical surface with respect to the center of the nascent cyst, and, as cysts grew, multiple apical membrane patches were detected within the same structure (Fig. 2E, lower panels). Counting cysts with single or multiple apical surfaces after 72 hours of culture, we found that the percentage of cysts with multiple apical surfaces was significantly higher in RPTP $\alpha$ -knockdown cells (55%) than in controls (22%) (Fig. 2F). We conclude that RPTP $\alpha$  knockdown leads to defective cyst morphogenesis in Caco-2 cells, and that this effect probably results from aberrant positioning of the apical compartment with respect to the growing cyst.

### RPTP $\alpha$ depletion impairs cadherin-based intercellular aggregation

Given the colocalization of RPTP $\alpha$  with E-cadherin, we speculated that the appearance of aberrant 3D structures resulting from RPTP $\alpha$  depletion might reflect a role for RPTP $\alpha$  in regulating the establishment and functions of E-cadherin-based adherens junctions. As a first step to address this possibility, we determined whether knockdown of RPTP $\alpha$  affected the ability of isolated Caco-2 cells to aggregate in suspension, a process that is promoted by homophilic E-cadherin adhesion (Nagafuchi et al., 1987). Control or RPTP $\alpha$ -depleted cells were incubated with shaking for 4 hours (Fig. 3A). At this time, control cells underwent calcium-dependent aggregation. By contrast, RPTP $\alpha$ -depleted cells tended to remain isolated or formed aggregates of reduced size compared with controls (Fig. 3B). We conclude that RPTP $\alpha$  knockdown compromises E-cadherin-mediated intercellular aggregation in suspension.

### RPTP $\alpha$ is necessary for the integrity of cell–cell contacts in epithelial cell monolayers

We subsequently analyzed the effect of transient knockdown of RPTP $\alpha$  on junctional morphology in monolayer culture. Transfection of siRNA reduced overall RPTP $\alpha$  levels in confluent Caco-2 cells by ~90% (Fig. 4A). RPTP $\alpha$  depletion perturbed E-cadherin staining (Fig. 4B, left panels), although it did not affect the total level of E-cadherin (Fig. 4A), suggesting defects in protein distribution at the cell membrane. Contrasting with the sharp and linear staining in control cells, reducing RPTP $\alpha$  levels induced a broadening of E-cadherin staining throughout the lateral cell–cell interface, with a discontinuous distribution. To quantify such alterations, we measured the width and average pixel intensity of E-cadherin staining at the cell–cell contacts. As shown in Fig. 4C, RPTP $\alpha$  knockdown was

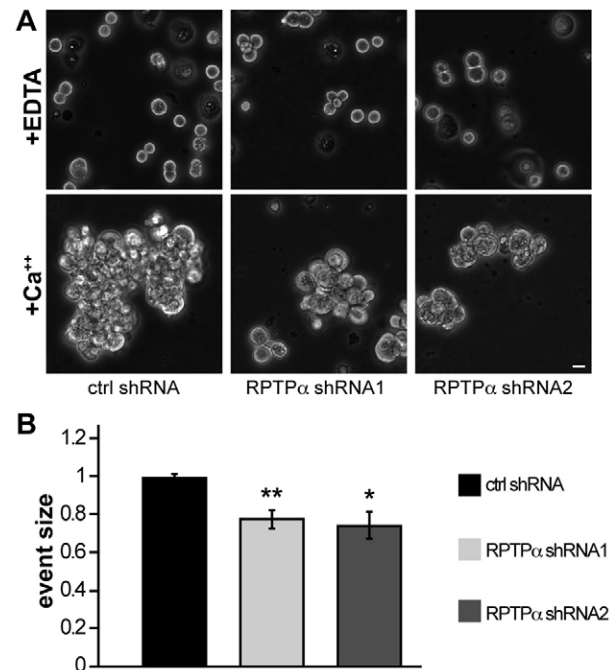


**Fig. 3. RPTP $\alpha$  is required for cell aggregation.** Control and RPTP $\alpha$ -depleted Caco-2 cells were isolated in presence of EDTA, incubated with shaking and analyzed for aggregate formation after 90 minutes. (A) Phase-contrast images of transduced Caco-2 cells expressing shRNA against human RPTP $\alpha$  (RPTP $\alpha$  shRNA1, shRNA2) or a non-targeting shRNA (ctrl shRNA) aggregated in the absence (+EDTA) or presence (+Ca<sup>++</sup>) of calcium. Scale bar: 20  $\mu$ m (B) Quantification of aggregate size. Data show the mean  $\pm$  s.e.m. (three independent experiments, in each of which five fields were analyzed). \* $P$ <0.05; \*\* $P$ <0.01.

associated with significantly broader E-cadherin staining and a significant reduction in average staining intensity at cell–cell contacts. The distribution of E-cadherin signal, measured along intercellular contacts, also revealed that the continuous staining in control cells was replaced by a more discontinuous signal in RPTP $\alpha$ -depleted cells. The peri-junctional actin cytoskeleton, linked with E-cadherin at the adherens junctions, was also greatly perturbed by RPTP $\alpha$  knockdown (Fig. 4B, middle panels). Whereas control cells showed an intense ring of F-actin at the interface between cells, RPTP $\alpha$ -knockdown cells showed reduced F-actin density at contacts (Fig. 4D). Both aberrant E-cadherin and F-actin distribution caused by RPTP $\alpha$  depletion could be rescued by expressing siRNA-resistant mouse RPTP $\alpha$  (Fig. 7C).

Contrasting with these observations, the integrity of tight junctions seemed not to be impaired by knockdown of RPTP $\alpha$ , as observed by staining with ZO-1 (Fig. 4B, right panels). However, RPTP $\alpha$  depletion reduced junctional linearity at the apical intercellular boundaries; following RPTP $\alpha$  knockdown, cell–cell junctions appeared more wavy and less straight compared with those of control cells (Fig. 4B, right panels; Fig. 4E), suggesting that loss of RPTP $\alpha$  reduces junctional tension (McLachlan and Yap, 2011; Otani et al., 2006). Similar junctional defects were observed when RPTP $\alpha$  was knocked down by using siRNA in the breast carcinoma cell line MCF7 (supplementary material Fig. S1). Taken together, our data indicate that RPTP $\alpha$  is required for the integrity and organization of E-cadherin-based intercellular junctions and the underlying actin cytoskeleton.

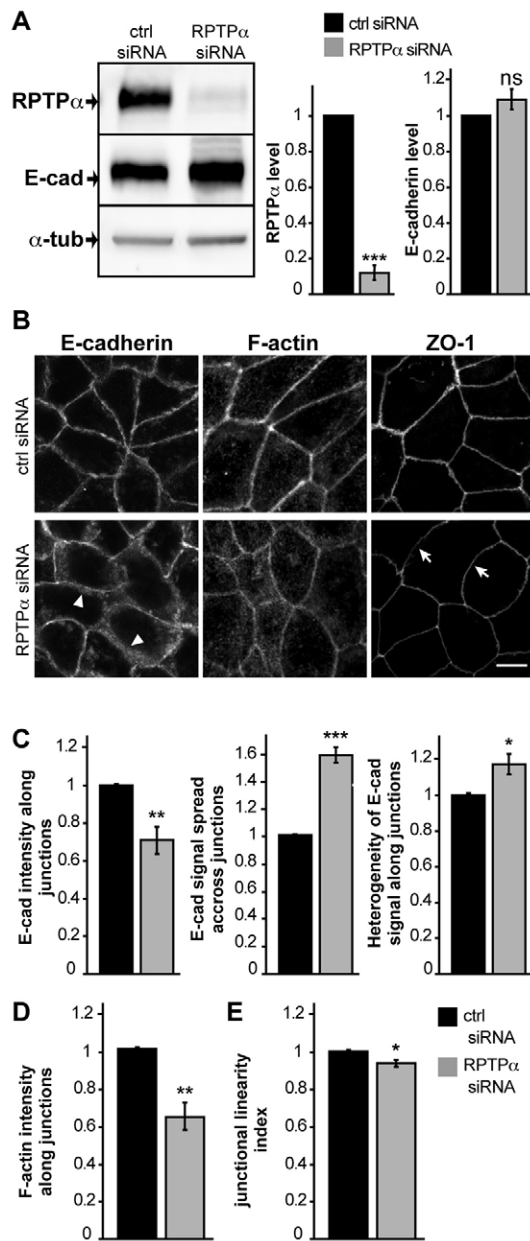


**Fig. 4. RPTP $\alpha$  is necessary for the integrity of junctions in epithelial cell monolayers.** Caco-2 cells were transiently transfected with siRNA against RPTP $\alpha$  (RPTP $\alpha$  siRNA) or with scrambled control RNA (ctrl siRNA), and analyzed at 72 hours after transfection. (A) Western blot analysis of RPTP $\alpha$  in both conditions (left panel). Densitometric quantification of RPTP $\alpha$  (middle panel) and E-cadherin (right panel) expression normalized to  $\alpha$ -tubulin is shown as the mean  $\pm$  s.e.m. (at least three independent experiments). (B) Immunofluorescence for E-cadherin (left panel), F-actin (middle panel) or ZO-1 (right panel) in control and RNAi-treated cells. Single z confocal pictures are shown. Arrowheads, abnormal distribution of E-cadherin; arrows, junctions showing loss of linearity. Scale bar: 10  $\mu$ m. (C) Quantification of the intensity and heterogeneity of E-cadherin signal along junctions, and the spread of E-cadherin signal across junctions. (D) Quantification of the peri-junctional F-actin intensity. (E) Quantification of the junctional linearity assessed by analysis of ZO-1 staining. Data show the mean  $\pm$  s.e.m. and are expressed relative to the control (three independent transfections, for each of which >30 junctions were analyzed). \* $P$ <0.05; \*\* $P$ <0.01; \*\*\* $P$ <0.001; ns, non-significant.

### RPTP $\alpha$ is required for tonic Src activity in epithelial cells, and controls tyrosine phosphorylation at epithelial junctions

Tyrosine phosphorylation is crucial for both the assembly and stability of cadherin-based adhesive complexes. Broad-spectrum PTP inhibition using vanadate indicates that PTP activity is required for keeping a balanced phosphotyrosine content at cell–cell junctions, and for the maintenance of these structures (McLachlan and Yap, 2011). Decreased tyrosine phosphorylation upon PTP inhibition might reflect the ability of certain PTPs to positively modulate kinase activity and signaling (Burns et al., 1994; Su et al., 1999; McLachlan and Yap, 2011). Indeed, RPTP $\alpha$  is an established physiological activator of SFKs in multiple contexts, owing to its ability to dephosphorylate their inhibitory C-terminal residue (Su et al., 1999; Ponniah et al., 1999; Zheng et al., 2000; Bodrikov et al., 2005; Vacaresse et al., 2008). Because c-Src is present at cell–cell contacts, we checked whether RPTP $\alpha$  depletion might affect its kinase activity in epithelial cells. For this purpose, we used an antibody against phosphorylated tyrosine 419 (pY419-Src), an activation loop residue in c-Src, phosphorylation of which correlates with the active state. As shown in Fig. 5A,B, depletion of RPTP $\alpha$  significantly reduced the fraction of pY419-Src, by an extent (50–60%) comparable to that seen in other settings (Su et al., 1999; Ponniah et al., 1999; Zheng and Shalloway, 2001; Roskoski, 2005). We then compared the distribution of total protein tyrosine phosphorylation between control and RPTP $\alpha$ -depleted cells. Anti-phosphotyrosine immunostaining revealed a local decrease in tyrosine phosphorylation at cell–cell contacts following RPTP $\alpha$  knockdown (Fig. 5C,D). This decrease in junctional tyrosine phosphorylation was accompanied by a local decrease in c-Src activation – transient RPTP $\alpha$  knockdown reduced the fraction of Y419-phosphorylated c-Src at intercellular contacts (Fig. 5E,F). These findings reveal that RPTP $\alpha$  contributes to Src activity in epithelial cells, particularly at intercellular contacts, where, consequently, RPTP $\alpha$  is likely to promote tyrosine phosphorylation.

### RPTP $\alpha$ is required for E-cadherin-mediated Src activation

Cadherin-dependent cell–cell adhesion activates c-Src and other SFKs (McLachlan et al., 2007; Yap and Kovacs, 2003); however, the molecular mechanism of this process remains as yet unknown. Because our findings demonstrated that RPTP $\alpha$  is essential for Src activation in epithelial cells, we proceeded to test the involvement of RPTP $\alpha$  in early responses to E-cadherin-dependent cell adhesion. To this end, we homophilically activated E-cadherin at the surface of isolated cells using a recombinant ligand consisting of the ectodomain of human E-cadherin fused to the Fc moiety of IgG (Ecad–Fc) (Adams et al., 1996). This approach allowed us to isolate the effect of E-cadherin homophilic ligation from that of other juxtacrine signals that are exchanged during cell–cell contact (Yap and Kovacs, 2003).

Control and RPTP $\alpha$ -knockdown cells were allowed to adhere to substrata coated with Ecad–Fc for 90 minutes. We observed RPTP $\alpha$  specifically accumulating at the leading edge of control cells spreading on Ecad–Fc, whereas it was absent from the leading edge of RPTP $\alpha$ -knockdown cells (Fig. 6A). Wondering whether RPTP $\alpha$  accumulation at active leading edges might have a role in cadherin-based cellular spreading, we compared the extent of spreading of control and RPTP $\alpha$ -knockdown cells on Ecad–Fc-coated surfaces or surfaces coated with the non-signaling adhesive ligand poly-D-lysine (PDL). As expected (Kovacs et al., 2002b), cells did not spread on PDL-coated

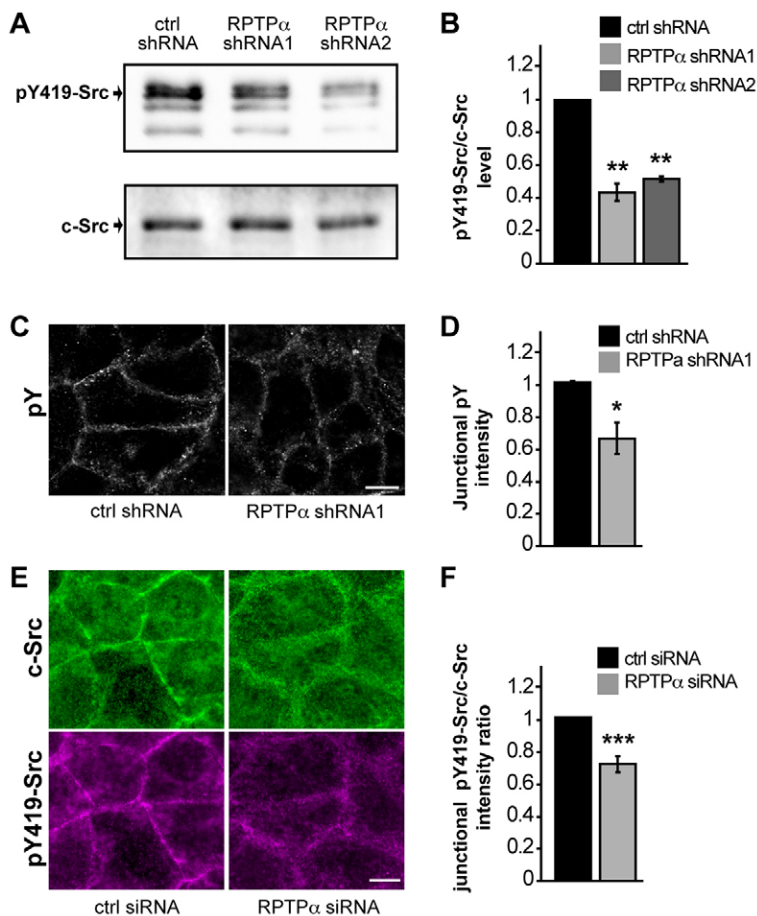


**Fig. 5. RPTP $\alpha$  is required for tonic Src activity in epithelial cells, and controls tyrosine phosphorylation at the epithelial junctions.** (A) Western blot analysis of activated c-Src (pY419-Src) and total c-Src (c-Src) in total cell extracts of Caco-2 cells expressing shRNAs against human RPTP $\alpha$  (RPTP $\alpha$  shRNA1 or RPTP $\alpha$  shRNA2) or a non-targeting shRNA (ctrl shRNA). (B) Densitometric quantification of pY419-Src levels relative to total c-Src levels. Data show the mean  $\pm$  s.e.m. (three experiments). (C) Immunofluorescence for total phosphotyrosine (pY) in control and stable RPTP $\alpha$ -knockdown cells. Scale bar: 10  $\mu$ m. (D) Quantification of phosphotyrosine signal intensity along junctions. Data show the mean  $\pm$  s.e.m. (three independent experiments, for each of which  $\geq 20$  junctions were analyzed). (E) Immunostaining for total c-Src (green) and activated c-Src (pY419-Src, purple) in Caco-2 cells transiently transfected with siRNA against RPTP $\alpha$  or with scrambled control RNA. Scale bar: 10  $\mu$ m. (F) Quantification of relative pY419-Src versus c-Src signal intensity along junctions. Data show the ratio of intensities of the two signals, represented as the mean  $\pm$  s.e.m.; a representative of two experiments is shown; 200 junctions were analyzed. \* $P < 0.05$ ; \*\* $P < 0.01$ ; \*\*\* $P < 0.001$ .

surfaces, but engaged in rapid spreading upon adhesion to substrate coated with recombinant E-cadherin, as revealed by the appearance of prominent lamellipodia (Fig. 6B). Spreading on Ecad-Fc was cadherin-dependent, as it was inhibited by an E-cadherin-blocking antibody (supplementary material Fig. S2A,B).

We then studied the involvement of RPTP $\alpha$  in spreading on Ecad-Fc. Strikingly, RPTP $\alpha$  depletion was associated with a spreading defect, because the total surface area of RPTP $\alpha$  knockdown cells was significantly reduced relative to that of controls for cells transfected with the most effective shRNA (RPTP $\alpha$  shRNA1), with a tendency towards a reduced area for cells transfected with the less effective shRNA2 (Fig. 6C). We previously showed that RPTP $\alpha$  associates with  $\alpha_v\beta_3$  integrin at the leading edge of cells spreading on vitronectin (von Wichert et al., 2003). To rule out interference by integrin-dependent effects during spreading on Ecad-Fc, we used the integrin-blocking peptide GPenGRGDSPCA (cRGD), an  $\alpha_v\beta_3$  antagonist. cRGD impaired the spreading of Caco-2 cells on fibronectin (supplementary material Fig. S2C), reflecting additional blocking of fibronectin-binding integrins, but did not change the decrease (by 35%) in spreading on Ecad-Fc of RPTP $\alpha$ -knockdown cells compared with that of controls (Fig. 6C; supplementary material Fig. S2E).

Previous studies have shown that adhesion to E-cadherin substrate stimulates the activation of SFKs (McLachlan et al., 2007). We therefore monitored the effect of RPTP $\alpha$  knockdown on E-cadherin-mediated Src activation. At 90 minutes after initial adhesion to recombinant cadherin, immunostaining for pY419-Src in control cells revealed active c-Src at the E-cadherin-driven

lamellipodia. By contrast, the ability of RPTP $\alpha$  shRNA1 cells to activate c-Src at these sites was compromised, as revealed by decreased pY419-Src staining at cadherin-based lamellipodia compared with that of controls, whereas the less effectively interfering shRNA2 caused a tendency towards decreased staining (Fig. 6D,E). Taken together, our observations provide evidence that RPTP $\alpha$  is required for the activation of Src downstream of E-cadherin.

#### RPTP $\alpha$ regulates cadherin-based junctions by affecting cortactin tyrosine phosphorylation

We wished to determine which of the multiple signaling events triggered by c-Src mediates RPTP $\alpha$ -dependent control of epithelial junctions. In previous studies, we have shown that the actin-binding protein cortactin is necessary for E-cadherin-mediated contact formation and actin reorganization, and that it is a target of E-cadherin-activated Src (Helwani et al., 2004; Ren et al., 2009). Cortactin depletion affects junctional E-cadherin accumulation, and rescue of this phenotype requires tyrosine phosphorylation of cortactin (Ren et al., 2009). We observed the presence of cortactin in an *in vitro* pull-down assay from Caco-2 cells aimed at characterizing interaction partners and substrates for RPTP $\alpha$  (supplementary material Fig. S3). These observations led us to investigate the functional interaction between cortactin and RPTP $\alpha$  at epithelial junctions.

We first determined whether RPTP $\alpha$  depletion affects tyrosine phosphorylation of cortactin. Cortactin immunoprecipitation, followed by anti-phosphotyrosine immunoblotting, revealed reduced cortactin tyrosine phosphorylation in RPTP $\alpha$ -knockdown



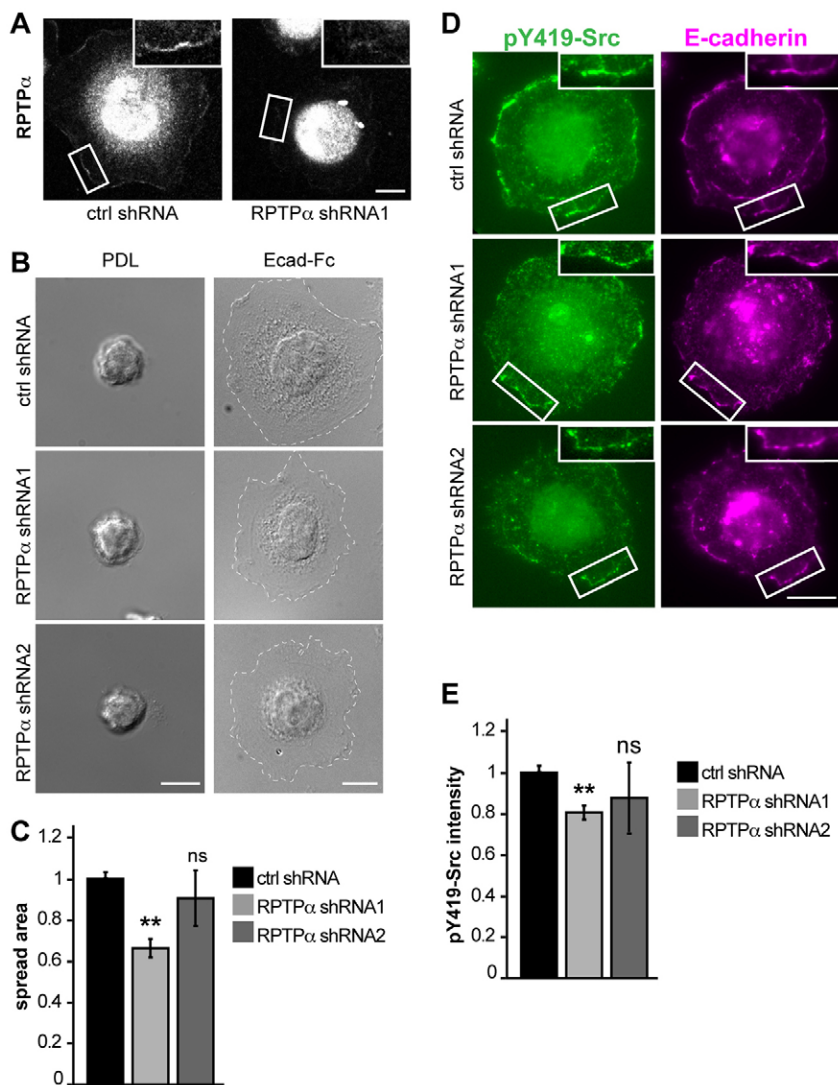


**Fig. 6. RPTP $\alpha$  is required for E-cadherin-dependent cell spreading and Src activation.** Cell spreading assay of Caco-2 cells expressing shRNAs against human RPTP $\alpha$  (RPTP $\alpha$  shRNA1 and shRNA2) or a non-targeting shRNA (ctrl shRNA) on poly-D-lysine (PDL) or E-cadherin (Ecad-Fc)-coated surfaces. (A) Immunofluorescence for RPTP $\alpha$  in cells that were allowed to spread on Ecad-Fc for 90 minutes. Single z confocal pictures are shown. Higher magnifications of cadherin-driven lamellipodia (white boxes) are shown in the upper-right corner of each image. Scale bar: 10  $\mu$ m. (B) Representative phase-contrast images of control and RPTP $\alpha$ -knockdown spreading cells. A dashed line delimits the surface area in contact with the substrate. Scale bars: 10  $\mu$ m. (C) Quantification of the cell surface area in contact with the Ecad-Fc-coated substrate is expressed as the mean  $\pm$  s.e.m. (three independent experiments, for each of which  $\geq 60$  cells were analyzed). (D) Co-immunofluorescence for activated c-Src (pY419-Src, green) and E-cadherin (purple) in cells that were allowed to spread on Ecad-Fc for 90 minutes (in presence of the RGD peptide). Higher magnifications of cadherin-driven lamellipodia (white boxes) are shown in the upper-right corner of each image. Scale bar: 10  $\mu$ m. (E) Quantification of the pY419-Src signal intensity measured at the cadherin-based lamellipodia of single cells spreading on Ecad-Fc (in the presence of the RGD peptide). Data show the mean  $\pm$  s.e.m. (three independent experiments, for each of which  $\geq 9$  cells were analyzed). \*\* $P < 0.01$ ; ns, non-significant.

cells as compared with controls, whereas total cortactin recovery was comparable (Fig. 7A).

This finding suggested that cortactin might be a functional downstream effector of RPTP $\alpha$ -activated c-Src at cadherin-based junctions. To test this possibility, we examined how the expression of phosphorylation mutants of cortactin affected the junctional phenotype induced by RPTP $\alpha$  knockdown. Accordingly, we transfected Caco-2 cells with RPTP $\alpha$  siRNA, either alone or together with a number of cortactin variants – wild-type cortactin, a non-phosphorylatable variant (3YF, in which three principal tyrosine residues, Y421, Y470 and Y486, were mutated to phenylalanine) or a phosphomimetic variant (3YD, in which these three tyrosine residues were replaced with aspartic acid) (Ren et al., 2009) – or a fluorescently tagged mouse RPTP $\alpha$  construct (mRPTP $\alpha$ -Cherry). We subsequently monitored the intensity of E-cadherin signal and the density of F-actin along junctions as a measure of the junctional RPTP $\alpha$ -knockdown phenotype. Overexpression of either wild-type cortactin or the 3YF variant had no effect on the reduction in the levels of junctional E-cadherin and F-actin induced by RPTP $\alpha$  depletion. By contrast, expression of cortactin 3YD significantly increased junctional E-cadherin and F-actin in

RPTP $\alpha$ -knockdown cells to a level that was comparable to that observed when mRPTP $\alpha$  was used to rescue the phenotype (Fig. 7B–D). These results indicate that RPTP $\alpha$  knockdown reduces the tyrosine phosphorylation of cortactin, and suggest that this reduction is responsible for the perturbed junctional organization associated with RPTP $\alpha$  depletion.

## DISCUSSION

### RPTP $\alpha$ controls a c-Src–cortactin signaling pathway that is important for the organization of epithelial adherens junctions

Epithelial integrity and organization are collective cellular functions that accordingly require coordinated intercellular adhesion and communication, processes in which E-cadherin-mediated phosphotyrosine signaling by SFKs is crucial. The v-Src oncogene has long been known to disturb epithelial integrity, and, more recently, c-Src signaling was reported to be activated by E-cadherin homophilic binding and to mediate junctional organization (McLachlan et al., 2007). However, the factors that control c-Src at adherens junctions have hardly been identified. The tyrosine phosphatase RPTP $\alpha$  has been implicated in SFK regulation in fibroblasts, neurons and other cell types, by virtue

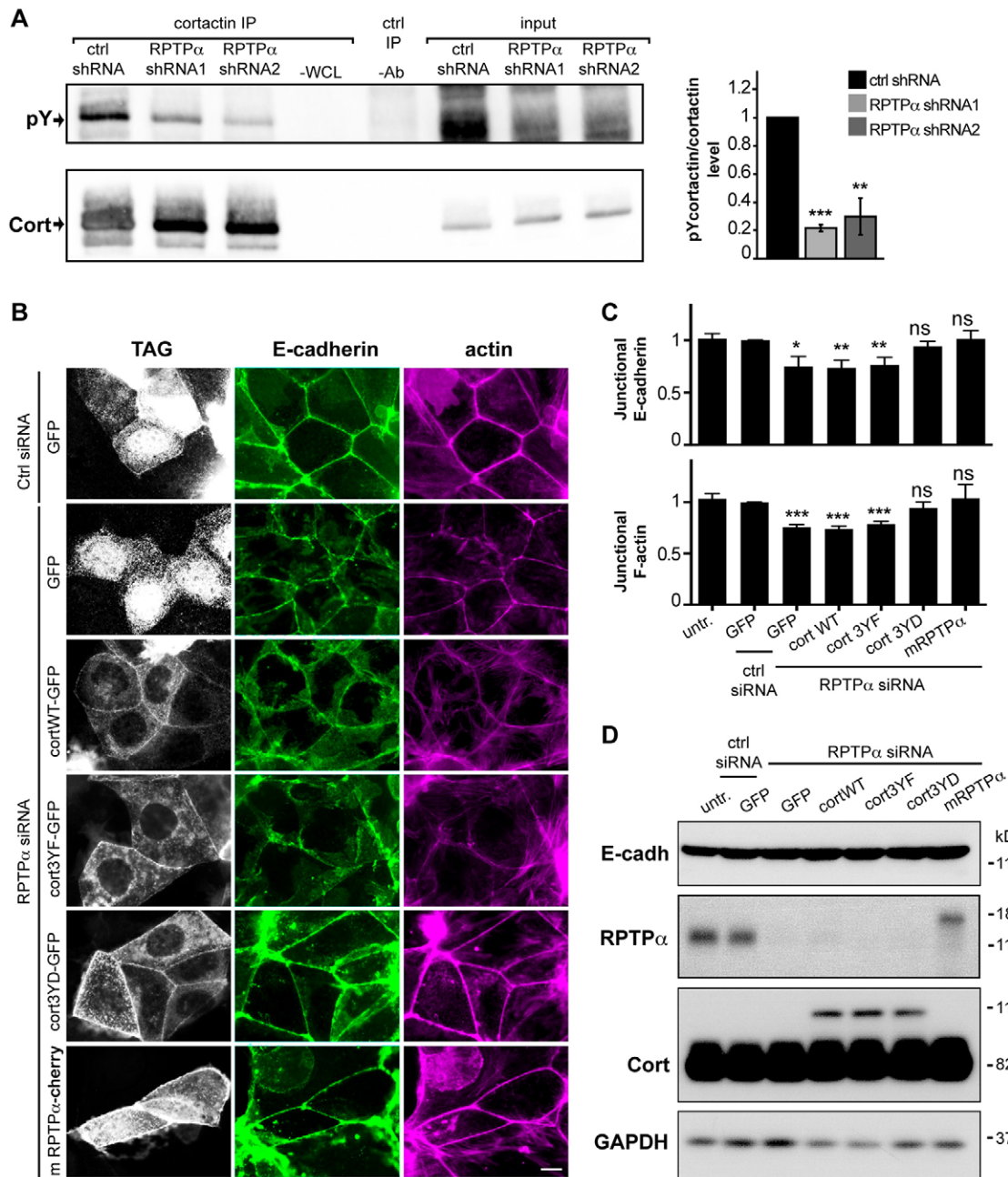


**Fig. 7. RPTP $\alpha$  regulates cadherin-based junctions by affecting tyrosine phosphorylation of cortactin.** (A) Analysis of cortactin tyrosine phosphorylation in Caco-2 cells expressing shRNAs against human RPTP $\alpha$  (RPTP $\alpha$  shRNA1 and shRNA2) or a non-targeting shRNA (ctrl shRNA). Left, cortactin was immunoprecipitated (IP) from cell lysates (input), and analyzed by immunoblotting with anti-phosphotyrosine (pY) or anti-cortactin (Cort). –WCL, no whole-cell lysate control; –Ab, no-antibody control. Right, densitometric quantification of pY-cortactin relative to total cortactin recovered after cortactin IP is shown as the mean  $\pm$  s.e.m. (five independent experiments). (B) Rescue of RPTP $\alpha$ -knockdown-induced junctional defects by overexpression of non-phosphorylatable versus phosphomimetic mutants of cortactin. Caco-2 cells transfected with siRNA against RPTP $\alpha$ , together with plasmids expressing GFP-tagged wild-type (cortWT–GFP) or mutated (cort3YF–GFP and cort3YD–GFP) human cortactin, or mouse RPTP $\alpha$  fused to Cherry (mRPTP $\alpha$ –Cherry) were fixed and immunostained for E-cadherin or F-actin. Representative confocal images show the distribution of the fluorescent tag (white), E-cadherin (green) or F-actin (purple) at intercellular junctions under the various conditions. Scale bar: 10  $\mu$ m. (C) Quantitative analysis of junctional E-cadherin (upper graph) or F-actin intensity (lower graph). untr., untreated controls. Data show the mean  $\pm$  s.e.m. (three independent experiments;  $n=21$ ). \* $P<0.05$ ; \*\* $P<0.01$ ; \*\*\* $P<0.001$ ; ns, non-significant. (D) Western blot analysis of E-cadherin (E-cadh), RPTP $\alpha$  and cortactin under the various conditions. The anti-GAPDH blot is shown as a loading control.

of its ability to specifically remove an inhibitory phosphate on the crucial regulatory C-terminal tyrosine residue in these kinases. In spite of the potential relevance of RPTP $\alpha$  in carcinomas (in which SFKs are commonly found to be

activated), the epithelial cell biology of RPTP $\alpha$  remained unexplored.

Here, we observe that RPTP $\alpha$  is enriched at cadherin-based adherens junctions, where it is in close molecular proximity to



E-cadherin, and that it participates in the activation and regulation of epithelial c-Src at this cellular locale. This effect is accompanied by control of the ability of epithelial cells to organize in well-ordered 3D structures, to form calcium-dependent aggregates and to maintain the integrity of intercellular junctions. In cellular monolayers, knockdown of RPTP $\alpha$  affects E-cadherin organization, the peri-junctional F-actin ring and the linearity of cell–cell junctions.

Here, we identify the c-Src substrate cortactin as a downstream effector of RPTP $\alpha$ -activated c-Src at cadherin-based junctions. The junctional effects of RPTP $\alpha$  knockdown are similar to those of cortactin depletion in MCF7 cells (Ren et al., 2009) and in Caco-2 cells (data not shown). Here, we show that adequate tyrosine phosphorylation of cortactin depends on RPTP $\alpha$ , and the expression of the 3YD mutant form of cortactin normalizes the aberrant E-cadherin distribution associated with loss of RPTP $\alpha$ . This reveals a molecular link between RPTP $\alpha$  and epithelial junction integrity. It is possible to interpret the behavior of the 3YD mutant as mimicking (c-Src-mediated) cortactin phosphorylation. Although this interpretation requires caution, given the significant structural differences between aspartic acid and phosphotyrosine, it is supported by the observation that the 3YF mutant did not rescue the effect of either cortactin or RPTP $\alpha$  depletion.

As a target of E-cadherin-activated SFK signaling (Helwani et al., 2004; Ren et al., 2009), cortactin is a positive regulator of the Arp2/3 complex, involved in control and homeostasis of branched actin filaments. By showing RPTP $\alpha$ -mediated regulation of the junctional cortactin pool, our studies thus implicate RPTP $\alpha$  in coordination between E-cadherin and the actin cytoskeleton, a crucial process for intercellular adhesion (Lambert et al., 2002; Thomas et al., 2013).

### Functions of RPTP $\alpha$ at the epithelial junctions

Our observations indicate that RPTP $\alpha$  depletion might reduce intercellular adhesion strengthening by the peri-junctional actin cytoskeleton, by deregulating cortactin function. This would lead to aberrant organization of E-cadherin at adherens junctions. However, the potential for additional targets of RPTP $\alpha$ -mediated Src signaling at epithelial junctions merits exploration. Junctional integrity requires cortical actomyosin contractility, which is promoted by E-cadherin homophilic binding and contributes to the extension and strengthening of E-cadherin-based adhesions, by generating tension along the junctions (Gomez et al., 2011). RPTP $\alpha$  has already been linked to cytoskeletal contractility and stress fiber formation at integrin-based focal adhesion sites; these effects depend on substrate stiffness and require RPTP $\alpha$ -mediated SFK activation (Krdija et al., 2010; von Wichert et al., 2003; Zeng et al., 2003). Our observation of reduced junctional linearity in epithelial monolayers as a consequence of RPTP $\alpha$  knockdown suggests that there is imbalanced junctional tension between adjacent cells. In this sense, an additional relevant target of RPTP $\alpha$  at epithelial junctions might be the nonmuscle myosin IIB, which is required for E-cadherin organization at intercellular contacts (Smutny et al., 2010), and is recruited to the adherens junction through SFK signaling (McLachlan and Yap, 2011).

Surface organization of E-cadherin also relies on dynamic endocytosis and/or recycling, dysfunction of which might contribute to the discontinuous and punctuated distribution of E-cadherin observed upon RPTP $\alpha$  knockdown. Potentially, by regulating c-Src, RPTP $\alpha$  could control events in the endocytic pathway, given the implication of the former in epithelial

E-cadherin endocytosis (Canel et al., 2010; Swaminathan and Cartwright, 2012) and in neuronal neurotransmitter receptor trafficking in neurons (Ohnishi et al., 2011).

The complex and multistep nature of junctional organization and maturation, though ill-understood, raises the question of the stage of maturation at which RPTP $\alpha$  action is most crucial. RPTP $\alpha$ -knockdown-induced defects in cell aggregation and spreading on Ecad-Fc suggest an early intervention of RPTP $\alpha$ , consistent with its early recruitment to cell–cell contacts. It will be informative to characterize in detail the contribution of RPTP $\alpha$  to the formation and fusion of transient junctional intermediates (spot-like adherens junctions; Yonemura et al., 1995) during junctional maturation, as well as its contribution to E-cadherin dynamics, e.g. basal-to-apical flow (Kametani and Takeichi, 2007), and to endocytic recycling. Finally, our data do not rule out epithelial functions of RPTP $\alpha$  beyond E-cadherin-mediated adhesion, e.g. the relevance of RPTP $\alpha$  for 3D organization into cysts might suggest a role in the maintenance of apicobasal polarity.

### PTPs and the integrity of cadherin-based junctions

Our findings confirm and expand understanding of the involvement of PTPs in cell–cell adhesion. Results from experiments involving global PTP inhibition had suggested that PTPs support cadherin-based junctional integrity (McLachlan and Yap, 2011). However, such effects might merely reflect indirect activation of tyrosine kinases that are negatively controlled by PTPs. By contrast, our findings directly implicate RPTP $\alpha$  in the integrity of adherens junctions. Several other PTPs also act at junctions (Anders et al., 2006; Espejo et al., 2010; Fuchs et al., 1996; Müller et al., 1999; Sheth et al., 2007). To the best of our knowledge, our study identifies RPTP $\alpha$  as the first PTP controlling c-Src signaling at cadherin-based adhesions. It is, however, not unlikely that additional PTPs will be found to contribute to c-Src activation at cell–cell contacts.

### Mechanistic aspects of E-cadherin–RPTP $\alpha$ interactions

Our results suggest that RPTP $\alpha$  is responsible for local activation of c-Src signaling upon E-cadherin engagement. It remains to be elucidated how signals from E-cadherin adhesion would be transduced to RPTP $\alpha$ . RPTP $\alpha$  has been reported to transduce signals from cell adhesion molecules, such as NCAM or integrin, by physically associating with them. The occurrence of FRET between RPTP $\alpha$  and E-cadherin indicates close proximity and the potential for direct interaction, although the low level of co-immunoprecipitation between the two proteins suggests that their interaction might be weak and/or transient. Such interaction might be mediated by the RPTP $\alpha$  ectodomain, similar to what has been claimed for the association of RPTP $\alpha$  with the neural adhesion molecule contactin (Zeng et al., 1999); in this case, homophilic engagement of E-cadherin itself might be able to transmit a conformational signal to the RPTP $\alpha$  ectodomain, resulting in altered RPTP $\alpha$  function. Alternatively, the association might involve intracellular interactions, analogous to that suggested for RPTP $\alpha$ –NCAM crosstalk (Bodrikov et al., 2005). The dynamics of RPTP $\alpha$  recruitment as an E-cadherin partner will likely be a rewarding topic for further study.

A second issue requiring further study concerns the possibility and mechanism of the local activation of RPTP $\alpha$  at epithelial junctions. Indeed, multiple regulatory mechanisms are known to control RPTP $\alpha$ , including dimerization, post-translational modifications (such as serine and tyrosine phosphorylation and

cysteine oxidation) and conformational changes (Groen et al., 2008; Jiang et al., 1999; Su et al., 1994; Zheng and Shalloway, 2001). Whether and how E-cadherin homophilic binding, and the presence of particular factors or conditions at adherens junctions, affects one or several of these processes is an interesting question for future research. The answers should also be instructive concerning the other types of adhesion molecules and junctions that rely on PTPs for appropriate function.

## MATERIALS AND METHODS

### Cell culture

Caco-2 cells were cultured in RPMI medium containing 10% fetal bovine serum (FBS), non-essential amino acids (Gibco), penicillin (100 units/ml) and streptomycin (100 µg/ml). MCF-7, A431 and HEK 293T cells were cultured in DMEM supplemented with 10% FBS, penicillin (100 units/ml) and streptomycin (100 µg/ml). For 3D growth, Caco-2 cells were trypsinized to obtain a single-cell suspension. A suspension of  $5.8 \times 10^4$  cells/ml was mixed with a solution containing 40% Matrigel (BD, 354230), 1 mg/ml type I collagen (Trevigen, 3440-100-01) and 0.02 M HEPES. Cells embedded in this Matrigel solution were plated into eight-well chamber slides (Becton Dickinson). The Matrigel matrix was allowed to solidify by incubation at 37°C for 30 minutes prior to the addition of medium. Medium was renewed every 3–4 days up to 14 days to follow cyst formation.

### Plasmids and siRNA cell transfection

Y421D/Y470D/Y486D (3YD) and Y421F/Y470/Y486F (3YF) cortactin mutants were generated by two-step PCR-based mutagenesis and introduced into pEGFP-N1 vector. RPTP $\alpha$  RNAi oligonucleotide duplex (SASI\_Hs01\_00169093) and scrambled control RNA (SIC001) were from Sigma. Transient DNA and siRNA transfections were performed using Lipofectamine 2000 or RNAiMAX (Invitrogen) according to the manufacturer's instructions (with a 3:1 ratio of Lipofectamine reagent:DNA, and a final concentration of 50 nM siRNA).

Human  $\beta$ -catenin-mCherry and murine RPTP $\alpha$ -mCherry were obtained by cloning the corresponding cDNA into pmCherry-N1 vector (Clontech). Similarly, murine E-cadherin-GFP was obtained by cloning the murine E-cadherin cDNA into pEGFP-N1 (Clontech; Smutny et al., 2011). mCherry-VAMP3 was a generous gift from Jenny Stow (Institute for Molecular Bioscience, Australia). The GFP-mCherry tandem construct was obtained by cloning the GFP coding sequence between the *NheI* and *XhoI* sites of pmCherry-N1.

### Generation of lentiviral particles and infection

cDNA encoding human RPTP $\alpha$  was fused at its C-terminus to the fluorescent protein Venus and introduced into a pLenti derivative. Infected A431 cells were selected with 10 µg/ml blasticidin for 10 days. To knockdown RPTP $\alpha$ , we used the pLKO.1-puro lentiviral vector (Sigma). The sense targeting sequences for human *PTPRA* were 5'-GGCGAAGAGAATACAGACTAT-3' (RPTP $\alpha$  shRNA1) and 5'-AGCCCTTCTGGAGCATTATCT-3' (RPTP $\alpha$  shRNA2), and the sequence of the non-targeting control was 5'-CAACAAGATGAAGAGCACCAA-3' (Sigma TRC1.5 clone SHC002). A second generation packaging system was used to produce virus. For production of virus, 5 µg of transfer vector was co-transfected together with 10 µg of pMD2G (VSV-G, Addgene 12259) and 5 µg of psPax2 (gag-pol, tat-rev; Addgene 12260) using calcium phosphate coprecipitation into HEK 293T cells seeded 24 hours before transfection. Supernatant containing viral particles was harvested at 48 hours post-transfection, and concentrated 100-fold by ultracentrifugation at 80,000 g for 2 hours at 4°C using the SW32 Ti rotor (Beckman). The viral pellet was resuspended in PBS and stored at -80°C. Infected cells were selected in 4 µg/ml puromycin for 10 days, then maintained in 2 µg/ml puromycin.

### Cell aggregation assay

Nearly confluent cells were isolated by calcium sequestration in 4 mM EDTA in Hanks' Balanced Salt Solution (HBSS; 40 mg/l KCl, 60 mg/l

KH<sub>2</sub>PO<sub>4</sub>, 8 g/l NaCl, 90 mg/l Na<sub>2</sub>HPO<sub>4</sub>•7H<sub>2</sub>O, 100 mg/l D-glucose). Isolated cells were resuspended at  $2 \times 10^5$  cells/ml in 10 mM calcium-supplemented medium or in the presence of 4 mM EDTA, plated onto culture dishes that had been previously coated with 2% bovine serum albumin (BSA), 10 mM CaCl<sub>2</sub> in HBSS overnight at 4°C, and further shaken at 75 rpm for 4 hours at 37°C to allow aggregation. Cells were fixed in 2% paraformaldehyde (PFA) and phase-contrast images were taken using an Upright Leica DMR inverted microscope.

### Antibodies

The primary antibodies used were mouse monoclonal anti-E-cadherin (BD Transduction Laboratories), mouse monoclonal HECD-1 against the E-cadherin ectodomain (a gift from Peggy Wheelock; Omaha, NE), mouse monoclonal anti-E-cadherin blocking antibody (SHE78-7, Invitrogen), mouse monoclonal anti-cortactin (4F11, Millipore), mouse anti-phosphotyrosine (4G10, hybridoma culture supernatant), mouse monoclonal anti-v-Src (327, Sigma-Aldrich), mouse monoclonal anti-c-Src (antibody 2-17, Sandilands et al., 2007), rabbit polyclonal anti-Tyr(P)-419-Src family (Cell Signaling Technology), mouse monoclonal anti- $\alpha$ -tubulin (Sigma-Aldrich), rabbit polyclonal anti-RPTP $\alpha$  (Su et al., 1999) and mouse monoclonal anti-ZO-1 (Invitrogen). The secondary antibodies used were goat anti-rabbit-IgG or anti-mouse-IgG conjugated to Alexa Fluor 488, 594 or 647 (Invitrogen) and donkey anti-mouse-IgG or anti-rabbit-IgG conjugated to Cy3 (Jackson ImmunoResearch).

### Extracts and immunoblot analysis

Protein extracts were prepared in Triton lysis buffer (50 mM HEPES pH 7.5, 150 mM NaCl, 1.5 mM MgCl<sub>2</sub>, 1 mM EDTA, 10% glycerol and 1% Triton X-100), containing 1 mM Na<sub>3</sub>VO<sub>4</sub>, 10 mM NaF, 4% Protease Inhibitor Cocktail (Roche) and 1 mM PMSF, and cleared at 14,000 g for 15 minutes. 20 µg of protein was resuspended in Laemmli buffer, resolved on 8% polyacrylamide gels and transferred to Immobilon membrane (Millipore). Membranes were blocked with 5% skimmed milk or 5% BSA in TBS for 1 hour at room temperature and incubated overnight at 4°C with primary antibody. Membranes were washed, incubated for 1 hour with secondary antibody coupled with horseradish peroxidase (Jackson ImmunoResearch) and revealed by enhanced chemiluminescence. When required, membranes were incubated in stripping buffer (62.5 mM Tris-HCl pH 6.8, 2% SDS, 100 mM  $\beta$ -mercaptoethanol) for 1 hour at 60°C under agitation and washed in TBS containing 0.1% Tween-20.

### Immunoprecipitation

Protein-G-agarose beads (50% slurry, Upstate-16266) coupled to anti-cortactin antibody were incubated with 1.5 mg of lysate overnight at 4°C on a rotating wheel. The beads were washed six times with Triton lysis buffer containing 1 mM Na<sub>3</sub>VO<sub>4</sub> and 10 mM NaF, and resuspended in Laemmli buffer. Co-immunoprecipitation of RPTP $\alpha$  and E-cadherin was performed using lysis buffer containing 20 mM HEPES pH 7.5, 150 mM NaCl, 0.5% NP-40, 50 mM KCl, 2 mM CaCl<sub>2</sub> plus protease and phosphatase inhibitors.

### Recombinant protein production and purification

Expression vector (pEE14 backbone) containing the extracellular region of human E-cadherin fused to the IgG Fc (Ecad-Fc) was transiently transfected into HEK 293T cells. The secreted protein was purified from conditioned medium by Protein-A-affinity chromatography. Protein samples were dialyzed at 4°C into calcium-containing storage buffer (50 mM Tris-HCl pH 7.4, 150 mM NaCl, 2 mM CaCl<sub>2</sub>).

### Cell spreading assay

IbidiTreat (Ibidi) eight-well microslides were coated with Ecad-Fc (50 µg/ml) or poly-D-lysine (0.1 mg/ml) overnight at 4°C, then blocked with 10 mg/ml BSA, 5 mM CaCl<sub>2</sub> in HBSS for 30 minutes, as described previously (Kovacs et al., 2002a). Control and RPTP $\alpha$ -knockdown cells were trypsinized for 5 minutes at 37°C and maintained in single-cell suspension ( $2 \times 10^5$  cells/ml in serum-containing medium) for 1 hour at 37°C under constant agitation. Where applicable, during the last

30 minutes in suspension, the E-cadherin-blocking antibody SHE78-7 or the integrin-blocking peptide GPenGRGDSPGA (cRGD) (Bachem H-3964) were introduced. The cell suspension was then seeded onto coated plates and incubated at 37°C for 90 minutes. Cells were fixed with 1% PFA for immunofluorescence or staining with 0.5% Cresyl Violet. The total cell surface area (in pixels) of adherent cells was determined on phase-contrast images obtained by using an Upright Leica DMR inverted microscope and was analyzed by using Metamorph or ImageJ.

### **In vitro substrate trapping**

Human *PTPRA* catalytic site cysteine residues 442 and 732 were simultaneously mutated to serine, yielding the C/S mutant cDNA. The intracellular domain of wild-type or mutant (C/S) *PTPRA* was subcloned as an *XmaIII-EcoRV* fragment (after blunting the *XmaIII* overhang with Klenow) into the *SmaI* site of pGEX3X. GST-fusion proteins were produced in BCL bacteria, purified using glutathione–Sepharose beads (GE Healthcare) and stored in bound form at –80°C.

Nearly confluent cells were subjected to pervanadate treatment for 20 minutes by adding 1 mM Na<sub>3</sub>VO<sub>4</sub> and 1 mM H<sub>2</sub>O<sub>2</sub> into the culture medium. Cell extracts were prepared in Triton lysis buffer containing 5 mM iodoacetic acid, 10 mM NaF, 4% Protease Inhibitor Cocktail (Roche) and 1 mM PMSF, further incubated at 4°C for 15 minutes with 10 mM dithiothreitol (BioChemika) to inactivate unreacted iodoacetic acid and then incubated with GST fusion proteins coupled to glutathione–Sepharose beads for 90 minutes at 4°C. Beads were washed four times with lysis buffer, resuspended in Laemmli buffer and boiled before SDS-PAGE was performed.

### **Immunofluorescence and image analysis**

For antibody penetration in 3D cultures, collagen was digested in 50 units/ml collagenase III for 15 minutes at room temperature prior to fixation in 4% PFA for 30 minutes, and immunofluorescence was performed as described previously (Jaffe et al., 2008). Otherwise, cells were grown on glass coverslips until confluence and fixed for 5–15 minutes with 1–4% PFA. For immunofluorescence using the anti-E-cadherin antibody, cells were permeabilized in 0.025% saponin for 30 minutes and blocked in 10% FBS, 0.025% saponin. For all other antibodies, cells were permeabilized with 0.3% Triton X-100 in PBS for 5 minutes and blocked with 0.5% BSA, 0.2% gelatin, 150 mM NaCl, 0.1% Triton X-100. Incubation with primary antibodies was performed overnight at 4°C. After washing, incubation with secondary antibodies was performed for 1 hour at room temperature. Nuclei were stained with DAPI (100 ng/ml, Sigma). Coverslips were mounted in Mowiol (Sigma).

Epi-illumination images were acquired with an Upright Leica DMR inverted microscope and a DFC Leica camera, an IX81 Olympus microscope and a Hamamatsu Orca-1 ER camera or with a Leica TCS SP5 AOBS Tandem resonant Scanner confocal microscope, where indicated. Images were analyzed with Metamorph or ImageJ software.

To analyze E-cadherin signal spread, intensity and continuity, or F-actin density at cell–cell contacts, the Line Scan function of Metamorph was used. Briefly, spreading of the E-cadherin signal was measured from the spread of the signal intensity plots along a 50 pixel line orthogonal to individual cell–cell contacts. Fluorescence intensity at cell–cell contacts was analyzed by drawing regions of interest (ROIs) covering individual cell–cell contacts and measuring the average total signal intensity (for E-cadherin or F-actin) and the distribution of the signal, as the intensity standard deviation (for E-cadherin) within it. The junctional linearity index was calculated as the ratio of the linear distance between intercellular vertices to the real junction length, as described previously (Otani et al., 2006), analyzing individual randomly picked junctions from ZO-1 images. pY419-Src and total c-Src signal intensity on monolayers was analyzed by measuring the mean signal intensity along the same line (10 pixels wide) covering individual junctions. The analysis of the activation status of c-Src at the cadherin-driven lamellipodia in the spreading assay was performed by drawing a line (15 pixels wide) covering the entire perimeter of individual spread cells and measuring the average pY419-Src signal intensity along the line. Colocalization analysis was performed on individual cell–cell contact z-axis views with the ImageJ plugin JacoP, using Costes' method with 100 randomization rounds.

For FRET analysis, Caco-2 cells were cultured on glass-bottomed dishes (Shengyou Biotechnology Co., China) and transiently transfected with pEGFP-N1, pmCherry-N1 and GFP–mCherry tandem construct, or co-transfected with E-cad–GFP and β-catenin–mCherry or RPTPα–mCherry or mCherry–VAMP3. Live cells were imaged at 48 hours post-transfection at 37°C on an LSM510 Meta Zeiss confocal microscope. During imaging, cells were incubated in HBSS supplemented with 10 mM HEPES pH 7.4 and 5 mM CaCl<sub>2</sub>. Images were acquired with a 63× oil-immersion objective (Plan Apochromat 1.4 NA, Zeiss) with a resolution of 0.14 μm/pixel. Donor and FRET channels were recorded by scanning using a 488-nm laser line and collecting the emission in the donor emission region (band pass 500–530 nm) and acceptor emission region (long pass 560 nm), respectively. In addition, the acceptor channel was collected by using the 546-nm laser line for excitation and collecting the emission in the acceptor emission regions. Images were acquired by sequential line acquisition.

For FRET measurements, the corrected FRET (cFRET) signal from images from the FRET channel was obtained on a pixel-by-pixel basis using the following equation (Grashoff et al., 2010; Ferrari et al., 2012);

$$\text{cFRET} = \text{FRET} - \text{dbt}(I_D) \times I_D - \text{abt}(I_A) \times I_A,$$

where FRET is the FRET channel image, and  $\text{dbt}(I_D)$  and  $\text{abt}(I_A)$  are the donor and acceptor bleed-through fractions expressed as functions of donor ( $I_D$ ) and acceptor ( $I_A$ ) intensities.  $\text{dbt}(I_D)$  and  $\text{abt}(I_A)$  functions and cFRET calculations were performed as described previously (Grashoff et al., 2010) using a custom-made MatLab routine (Ratheesh et al., 2012).

The FRET efficiency was calculated for those pixels located in the selected ROIs corresponding to the zonula adherens of cells, as identified by E-cad–GFP fluorescence signal, or the cell cytoplasm when FRET efficiency was determined for the GFP–mCherry tandem construct. FRET efficiency was calculated for every image using the following equation (Ferrari et al., 2012);

$$E = 1 - \frac{I_D}{I_D + \text{cFRET}}$$

### **Statistical analyses**

Statistical significance of the data was assessed by calculating the *P*-values using two-tailed Student's *t*-tests, except for FRET measurements where one-way ANOVA followed by Tukey's multiple comparisons test was used. Statistical data are shown as follows: ns, not significant ( $P > 0.05$ ); \* $P < 0.05$ ; \*\* $P < 0.01$ ; \*\*\* $P < 0.001$ ; \*\*\*\* $P < 0.0001$ .

### **Acknowledgements**

We thank Takeshi Sakurai (Kyoto University, Japan) for the RPTPα-venus lentiviral construct, Delphine Delacour (Institut Jacques Monod, Paris, France) for assistance with 3D assays, the ImagoSeine facility (Institut Jacques Monod, Paris, France) for advice and training regarding imaging, Barbara Nuñez (Biotech Research and Innovation Centre, Copenhagen, Denmark) and Robert McLachlan (Institute for Molecular Bioscience, Brisbane, Australia) for pilot experiments, and Sylvie Dufour (Institut Curie, Paris, France) for discussion. The anti-Src-2-17 antibody was a generous gift from Margaret Frame and Bryan Serrels (University of Edinburgh, UK), and HECD-1 was a gift from Peggy Wheelock, Omaha, NE, with permission of Masatoshi Takeichi. mCherry–VAMP3 was a generous gift from Jenny Stow (Institute for Molecular Bioscience, Brisbane, Australia). We thank the reviewers for highly constructive comments and suggestions.

### **Competing interests**

The authors declare no competing interests.

### **Author contributions**

M.T., X.L., F.N., S.P.H. and G.A.G. performed experiments. N.V. made the initial observations. A.S.Y. and J.S. conceived the study. V.D. supervised much of the experimental work, and conceived and performed experiments. M.T., A.S.Y., G.A.G., V.D. and J.S. wrote the manuscript.

### **Funding**

Work was supported by Kræftens Bekæmpelse (Denmark); La Ligue contre le Cancer (France); the Australian Research Council; National Health & Medical Research Council of Australia [grant numbers 631683, APP1044041, APP1010489]; and Kids Cancer Project of the Oncology Research Foundation.



## Supplementary material

Supplementary material available online at  
<http://jcs.biologists.org/lookup/suppl/doi:10.1242/jcs.134379/-DC1>

## References

- Adams, C. L., Nelson, W. J. and Smith, S. J. (1996). Quantitative analysis of cadherin-catenin-actin reorganization during development of cell-cell adhesion. *J. Cell Biol.* **135**, 1899–1911.
- Anders, L., Mertins, P., Lammich, S., Murgia, M., Hartmann, D., Saftig, P., Haass, C. and Ullrich, A. (2006). Furin-, ADAM 10-, and gamma-secretase-mediated cleavage of a receptor tyrosine phosphatase and regulation of beta-catenin's transcriptional activity. *Mol. Cell Biol.* **26**, 3917–3934.
- Ardini, E., Agresti, R., Tagliabue, E., Greco, M., Aiello, P., Yang, L. T., Ménard, S. and Sap, J. (2000). Expression of protein tyrosine phosphatase alpha (RPTPalpa) in human breast cancer correlates with low tumor grade, and inhibits tumor cell growth in vitro and in vivo. *Oncogene* **19**, 4979–4987.
- Behrens, J., Vakaet, L., Friis, R., Winterhager, E., Van Roy, F., Mareel, M. M. and Birchmeier, W. (1993). Loss of epithelial differentiation and gain of invasiveness correlates with tyrosine phosphorylation of the E-cadherin/beta-catenin complex in cells transformed with a temperature-sensitive v-SRC gene. *J. Cell Biol.* **120**, 757–766.
- Bodrikov, V., Leshchyns'ka, I., Sytnyk, V., Overvoorde, J., den Hertog, J. and Schachner, M. (2005). RPTPalpa is essential for NCAM-mediated p59fyn activation and neurite elongation. *J. Cell Biol.* **168**, 127–139.
- Braga, V. M. and Yap, A. S. (2005). The challenges of abundance: epithelial junctions and small GTPase signalling. *Curr. Opin. Cell Biol.* **17**, 466–474.
- Burns, C. M., Sakaguchi, K., Appella, E. and Ashwell, J. D. (1994). CD45 regulation of tyrosine phosphorylation and enzyme activity of src family kinases. *J. Biol. Chem.* **269**, 13594–13600.
- Calautti, E., Cabodi, S., Stein, P. L., Hatzfeld, M., Kedersha, N. and Paolo Dotto, G. (1998). Tyrosine phosphorylation and src family kinases control keratinocyte cell-cell adhesion. *J. Cell Biol.* **141**, 1449–1465.
- Canel, M., Serrels, A., Miller, D., Timpson, P., Serrels, B., Frame, M. C. and Brunton, V. G. (2010). Quantitative in vivo imaging of the effects of inhibiting integrin signaling via Src and FAK on cancer cell movement: effects on E-cadherin dynamics. *Cancer Res.* **70**, 9413–9422.
- Espejo, R., Rengifo-Cam, W., Schaller, M. D., Evers, B. M. and Sastry, S. K. (2010). PTP-PEST controls motility, adherens junction assembly, and Rho GTPase activity in colon cancer cells. *Am. J. Physiol.* **299**, C454–C463.
- Ferrari, M. L., Gomez, G. A. and Maccioni, H. J. (2012). Spatial organization and stoichiometry of N-terminal domain-mediated glycosyltransferase complexes in Golgi membranes determined by fret microscopy. *Neurochem. Res.* **37**, 1325–1334.
- Fuchs, M., Müller, T., Lerch, M. M. and Ullrich, A. (1996). Association of human protein-tyrosine phosphatase kappa with members of the armadillo family. *J. Biol. Chem.* **271**, 16712–16719.
- Gomez, G. A., McLachlan, R. W. and Yap, A. S. (2011). Productive tension: force-sensing and homeostasis of cell-cell junctions. *Trends Cell Biol.* **21**, 499–505.
- Grashoff, C., Hoffman, B. D., Brenner, M. D., Zhou, R., Parsons, M., Yang, M. T., McLean, M. A., Sligar, S. G., Chen, C. S., Ha, T. et al. (2010). Measuring mechanical tension across vinculin reveals regulation of focal adhesion dynamics. *Nature* **466**, 263–266.
- Groen, A., Overvoorde, J., van der Wijk, T. and den Hertog, J. (2008). Redox regulation of dimerization of the receptor protein-tyrosine phosphatases RPTPalpa, LAR, RPTPmu and CD45. *FEBS J.* **275**, 2597–2604.
- Gumbiner, B. M. (2005). Regulation of cadherin-mediated adhesion in morphogenesis. *Nat. Rev. Mol. Cell Biol.* **6**, 622–634.
- Halbleib, J. M. and Nelson, W. J. (2006). Cadherins in development: cell adhesion, sorting, and tissue morphogenesis. *Genes Dev.* **20**, 3199–3214.
- Harris, T. J. C. and Tepass, U. (2010). Adherens junctions: from molecules to morphogenesis. *Nat. Rev. Mol. Cell Biol.* **11**, 502–514.
- Helwani, F. M., Kovacs, E. M., Paterson, A. D., Verma, S., Ali, R. G., Fanning, A. S., Weed, S. A. and Yap, A. S. (2004). Cortactin is necessary for E-cadherin-mediated contact formation and actin reorganization. *J. Cell Biol.* **164**, 899–910.
- Huang, J., Yao, L., Xu, R., Wu, H., Wang, M., White, B. S., Shalloway, D. and Zheng, X. (2011). Activation of Src and transformation by an RPTP $\alpha$  splice mutant found in human tumours. *EMBO J.* **30**, 3200–3211.
- Jaffe, A. B., Kaji, N., Durgan, J. and Hall, A. (2008). Cdc42 controls spindle orientation to position the apical surface during epithelial morphogenesis. *J. Cell Biol.* **183**, 625–633.
- Jiang, G., den Hertog, J., Su, J., Noel, J., Sap, J. and Hunter, T. (1999). Dimerization inhibits the activity of receptor-like protein-tyrosine phosphatase-alpha. *Nature* **401**, 606–610.
- Jiang, G., Huang, A. H., Cai, Y., Tanase, M. and Sheetz, M. P. (2006). Rigidity sensing at the leading edge through alphavbeta3 integrins and RPTPalpa. *Biophys. J.* **90**, 1804–1809.
- Kametani, Y. and Takeichi, M. (2007). Basal-to-apical cadherin flow at cell junctions. *Nat. Cell Biol.* **9**, 92–98.
- Kovacs, E. M., Ali, R. G., McCormack, A. J. and Yap, A. S. (2002a). E-cadherin homophilic ligation directly signals through Rac and phosphatidylinositol 3-kinase to regulate adhesive contacts. *J. Biol. Chem.* **277**, 6708–6718.
- Kovacs, E. M., Goodwin, M., Ali, R. G., Paterson, A. D. and Yap, A. S. (2002b). Cadherin-directed actin assembly: E-cadherin physically associates with the Arp2/3 complex to direct actin assembly in nascent adhesive contacts. *Curr. Biol.* **12**, 379–382.
- Krndija, D., Schmid, H., Eismann, J.-L., Lother, U., Adler, G., Oswald, F., Seufferlein, T. and von Wichert, G. (2010). Substrate stiffness and the receptor-type tyrosine-protein phosphatase alpha regulate spreading of colon cancer cells through cytoskeletal contractility. *Oncogene* **29**, 2724–2738.
- Labbé, D. P., Hardy, S. and Tremblay, M. L. (2012). Protein tyrosine phosphatases in cancer: friends and foes! *Prog. Mol. Biol. Transl. Sci.* **106**, 253–306.
- Lambert, M., Choquet, D. and Mège, R.-M. (2002). Dynamics of ligand-induced, Rac1-dependent anchoring of cadherins to the actin cytoskeleton. *J. Cell Biol.* **157**, 469–479.
- Maher, P. A., Pasquale, E. B., Wang, J. Y. and Singer, S. J. (1985). Phosphotyrosine-containing proteins are concentrated in focal adhesions and intercellular junctions in normal cells. *Proc. Natl. Acad. Sci. USA* **82**, 6576–6580.
- McLachlan, R. W. and Yap, A. S. (2007). Not so simple: the complexity of phosphotyrosine signaling at cadherin adhesive contacts. *J. Mol. Med.* **85**, 545–554.
- McLachlan, R. W. and Yap, A. S. (2011). Protein tyrosine phosphatase activity is necessary for E-cadherin-activated Src signaling. *Cytoskeleton (Hoboken)* **68**, 32–43.
- McLachlan, R. W., Kraemer, A., Helwani, F. M., Kovacs, E. M. and Yap, A. S. (2007). E-cadherin adhesion activates c-Src signaling at cell-cell contacts. *Mol. Biol. Cell* **18**, 3214–3223.
- Mège, R.-M., Gavard, J. and Lambert, M. (2006). Regulation of cell-cell junctions by the cytoskeleton. *Curr. Opin. Cell Biol.* **18**, 541–548.
- Meyer, D. S., Aceto, N., Sausgruber, N., Brinkhaus, H., Müller, U., Pallen, C. J. and Bentires-Alj, M. (2013). Tyrosine phosphatase PTPalpha contributes to HER2-evoked breast tumor initiation and maintenance. *Oncogene* **14**, 398–402. doi:10.1038/onc.2012.585
- Müller, T., Choidas, A., Reichmann, E. and Ullrich, A. (1999). Phosphorylation and free pool of beta-catenin are regulated by tyrosine kinases and tyrosine phosphatases during epithelial cell migration. *J. Biol. Chem.* **274**, 10173–10183.
- Nagafuchi, A., Shirayoshi, Y., Okazaki, K., Yasuda, K. and Takeichi, M. (1987). Transformation of cell adhesion properties by exogenously introduced E-cadherin cDNA. *Nature* **329**, 341–343.
- Nagai, T., Ibata, K., Park, E. S., Kubota, M., Mikoshiba, K. and Miyawaki, A. (2002). A variant of yellow fluorescent protein with fast and efficient maturation for cell-biological applications. *Nat. Biotechnol.* **20**, 87–90.
- Nelson, W. J. (2008). Regulation of cell-cell adhesion by the cadherin-catenin complex. *Biochem. Soc. Trans.* **36**, 149–155.
- Nishimura, T. and Takeichi, M. (2009). Remodeling of the adherens junctions during morphogenesis. *Curr. Top. Dev. Biol.* **89**, 33–54.
- Ohnishi, H., Murata, Y., Okazawa, H. and Matozaki, T. (2011). Src family kinases: modulators of neurotransmitter receptor function and behavior. *Trends Neurosci.* **34**, 629–637.
- Otani, T., Ichii, T., Aono, S. and Takeichi, M. (2006). Cdc42 GEF Tuba regulates the junctional configuration of simple epithelial cells. *J. Cell Biol.* **175**, 135–146.
- Ponniah, S., Wang, D. Z., Lim, K. L. and Pallen, C. J. (1999). Targeted disruption of the tyrosine phosphatase PTPalpha leads to constitutive downregulation of the kinases Src and Fyn. *Curr. Biol.* **9**, 535–538.
- Ratheesh, A., Gomez, G. A., Priya, R., Verma, S., Kovacs, E. M., Jiang, K., Brown, N. H., Akhmanova, A., Stehbens, S. J. and Yap, A. S. (2012). Centralspindlin and  $\alpha$ -catenin regulate Rho signalling at the epithelial zonula adherens. *Nat. Cell Biol.* **14**, 818–828.
- Ren, G., Helwani, F. M., Verma, S., McLachlan, R. W., Weed, S. A. and Yap, A. S. (2009). Cortactin is a functional target of E-cadherin-activated Src family kinases in MCF7 epithelial monolayers. *J. Biol. Chem.* **284**, 18913–18922.
- Roskoski, R., Jr (2005). Src kinase regulation by phosphorylation and dephosphorylation. *Biochem. Biophys. Res. Commun.* **331**, 1–14.
- Sandilands, E., Brunton, V. G. and Frame, M. C. (2007). The membrane targeting and spatial activation of Src, Yes and Fyn is influenced by palmitoylation and distinct RhoB/RhoD endosome requirements. *J. Cell Sci.* **120**, 2555–2564.
- Sheth, P., Seth, A., Atkinson, K. J., Gheyi, T., Kale, G., Giorgianni, F., Desiderio, D. M., Li, C., Naren, A. and Rao, R. (2007). Acetaldehyde dissociates the PTP1B-E-cadherin-beta-catenin complex in Caco-2 cell monolayers by a phosphorylation-dependent mechanism. *Biochem. J.* **402**, 291–300.
- Smutny, M., Cox, H. L., Leerberg, J. M., Kovacs, E. M., Conti, M. A., Ferguson, C., Hamilton, N. A., Parton, R. G., Adelstein, R. S. and Yap, A. S. (2010). Myosin II isoforms identify distinct functional modules that support integrity of the epithelial zonula adherens. *Nat. Cell Biol.* **12**, 696–702.
- Smutny, M., Wu, S. K., Gomez, G. A., Mangold, S., Yap, A. S. and Hamilton, N. A. (2011). Multicomponent analysis of junctional movements regulated by myosin II isoforms at the epithelial zonula adherens. *PLoS ONE* **6**, e22458.
- Su, J., Batzer, A. and Sap, J. (1994). Receptor tyrosine phosphatase R-PTP-alpha is tyrosine-phosphorylated and associated with the adaptor protein Grb2. *J. Biol. Chem.* **269**, 18731–18734.
- Su, J., Muranjan, M. and Sap, J. (1999). Receptor protein tyrosine phosphatase alpha activates Src-family kinases and controls integrin-mediated responses in fibroblasts. *Curr. Biol.* **9**, 505–511.

- Swaminathan, G. and Cartwright, C. A.** (2012). Rack1 promotes epithelial cell-cell adhesion by regulating E-cadherin endocytosis. *Oncogene* **31**, 376–389.
- Takahashi, M., Takahashi, F., Ui-Tei, K., Kojima, T. and Saigo, K.** (2005). Requirements of genetic interactions between Src42A, armadillo and shotgun, a gene encoding E-cadherin, for normal development in *Drosophila*. *Development* **132**, 2547–2559.
- Thomas, W. A., Boscher, C., Chu, Y.-S., Cuvelier, D., Martinez-Rico, C., Seddiki, R., Heysch, J., Ladoux, B., Thiery, J. P., Mege, R.-M. et al.** (2013).  $\alpha$ -Catenin and vinculin cooperate to promote high E-cadherin-based adhesion strength. *J. Biol. Chem.* **288**, 4957–4969.
- Tremper-Wells, B., Resnick, R. J., Zheng, X., Holsinger, L. J. and Shalloway, D.** (2010). Extracellular domain dependence of PTPalpha transforming activity. *Genes Cells* **15**, 711–724.
- Vacaresse, N., Møller, B., Danielsen, E. M., Okada, M. and Sap, J.** (2008). Activation of c-Src and Fyn kinases by protein-tyrosine phosphatase RPTPalpha is substrate-specific and compatible with lipid raft localization. *J. Biol. Chem.* **283**, 35815–35824.
- Volberg, T., Geiger, B., Dror, R. and Zick, Y.** (1991). Modulation of intercellular adherens-type junctions and tyrosine phosphorylation of their components in RSV-transformed cultured chick lens cells. *Cell Regul.* **2**, 105–120.
- von Wichert, G., Jiang, G., Kostic, A., De Vos, K., Sap, J. and Sheetz, M. P.** (2003). RPTP-alpha acts as a transducer of mechanical force on alpha5/beta3-integrin-cytoskeleton linkages. *J. Cell Biol.* **161**, 143–153.
- Warren, S. L. and Nelson, W. J.** (1987). Nonmitogenic morphoregulatory action of pp60v-src on multicellular epithelial structures. *Mol. Cell. Biol.* **7**, 1326–1337.
- Yap, A. S. and Kovacs, E. M.** (2003). Direct cadherin-activated cell signaling: a view from the plasma membrane. *J. Cell Biol.* **160**, 11–16.
- Ye, H., Tan, Y. L. J., Ponniah, S., Takeda, Y., Wang, S.-Q., Schachner, M., Watanabe, K., Pallen, C. J. and Xiao, Z.-C.** (2008). Neural recognition molecules CHL1 and NB-3 regulate apical dendrite orientation in the neocortex via PTP alpha. *EMBO J.* **27**, 188–200.
- Yonemura, S., Itoh, M., Nagafuchi, A. and Tsukita, S.** (1995). Cell-to-cell adherens junction formation and actin filament organization: similarities and differences between non-polarized fibroblasts and polarized epithelial cells. *J. Cell Sci.* **108**, 127–142.
- Zeng, L., D'Alessandri, L., Kalousek, M. B., Vaughan, L. and Pallen, C. J.** (1999). Protein tyrosine phosphatase alpha (PTPalpha) and contactin form a novel neuronal receptor complex linked to the intracellular tyrosine kinase fyn. *J. Cell Biol.* **147**, 707–714.
- Zeng, L., Si, X., Yu, W.-P., Le, H. T., Ng, K. P., Teng, R. M. H., Ryan, K., Wang, D. Z.-M., Ponniah, S. and Pallen, C. J.** (2003). PTP alpha regulates integrin-stimulated FAK autophosphorylation and cytoskeletal rearrangement in cell spreading and migration. *J. Cell Biol.* **160**, 137–146.
- Zheng, X. M. and Shalloway, D.** (2001). Two mechanisms activate PTPalpha during mitosis. *EMBO J.* **20**, 6037–6049.
- Zheng, X. M., Wang, Y. and Pallen, C. J.** (1992). Cell transformation and activation of pp60c-src by overexpression of a protein tyrosine phosphatase. *Nature* **359**, 336–339.
- Zheng, X. M., Resnick, R. J. and Shalloway, D.** (2000). A phosphotyrosine displacement mechanism for activation of Src by PTPalpha. *EMBO J.* **19**, 964–978.